



MAX-PLANCK-GESELLSCHAFT

Christine Nowakowski, Patrick Kürschner
Peter Eberhard, Peter Benner

**Model Reduction of an Elastic Crankshaft
for Elastic Multibody Simulations**



**Max Planck Institute Magdeburg
Preprints**

MPIMD/12-07

March 19, 2012

Impressum:

Max Planck Institute for Dynamics of Complex Technical Systems, Magdeburg

Publisher:

Max Planck Institute for Dynamics of
Complex Technical Systems

Address:

Max Planck Institute for Dynamics of
Complex Technical Systems
Sandtorstr. 1
39106 Magdeburg

www.mpi-magdeburg.mpg.de/preprints

Model Reduction of an Elastic Crankshaft for Elastic Multibody Simulations

Christine Nowakowski*, Patrick Kürschner†, Peter Eberhard*, Peter Benner†

Abstract

System analysis and optimization of combustion engines and engine components are increasingly supported by digital simulations. In the simulation process of combustion engines multi physics simulations are used. As an example, in the simulation of a crank drive the mechanical subsystem is coupled to a hydrodynamic subsystem. As far as the modeling of the mechanical subsystems is concerned, elastic multibody systems are frequently used. During the simulation many equations must be solved simultaneously, the hydrodynamic equations as well as the equations of motion of each body in the elastic multibody system. Since the discretization of the elastic bodies, e.g. with the help of the finite element method, introduces a large number of elastic degrees of freedom, an efficient simulation of the system becomes difficult. The linear model reduction of the elastic degrees of freedom is a key step for using flexible bodies in multibody systems and turning simulations more efficient from a computational point of view. In recent years a variety of new reduction methods alongside the traditional techniques were developed in applied mathematics. Some of these methods are introduced and compared for reducing the equations of motion of an elastic multibody system. The special focus of this work is on balanced truncation model order reduction which is a singular value based reduction technique using the Gramian matrices of the system. We investigate a version of this method that is adapted to the structure of a special class of second order dynamical systems which is important for the particular application discussed here. The main computational task in balanced truncation is the solution of large-scale Lyapunov equations for which we apply a modified variant of the low-rank ADI method. The simulation of a crank drive with a flexible crankshaft is taken as technically relevant example. The results are compared to other methods like Krylov approaches or modal reduction.

I. INTRODUCTION

One important step in the development process of technical products is the digital engineering using computer aided simulations. In this way many experiments and prototypes, and hence financial costs can be saved. Coupled simulations of different physical areas have become increasingly important as described in [3]. The efficient simulation of such systems, e.g. consisting of mechanical, electrical, hydraulic or pneumatic components, is of utmost interest. With respect to the growing working speeds and usage of lightweight structures, elastic multibody systems (EMBS) can be frequently used for the dynamical simulation of the mechanical parts. For systems where the elastic deformation is small compared to the rigid body motion, the floating frame of reference method is a sensible choice for the description of flexible bodies. The basic idea is to divide the movement of a body into a large nonlinearly described motion of the reference system and in a linear elastic deformation with respect to the reference system. Usually, the finite element method (FEM) is used for the modeling of the elastic deformations. Thereby, a very large number of elastic degrees of freedom is introduced into the model. One essential step for an efficient simulation of EMBS is the reduction of the linear elastic degrees of freedom, see [32], [21]. Currently, reduction techniques based on modal reduction, condensation and component mode synthesis (CMS) are often used in industrial environments. A variety of reduction techniques based on moment-matching with Krylov subspaces [26] or singular value decompositions (SVD) [37] have been developed in the last years in addition to the traditional approaches. An overview about the current state of development can be found e.g. in [2], [46]. These modern strategies often yield a more accurate approximation of the system dynamics with the same dimension of the reduced order model, or a comparable accuracy with smaller reduced order models, as obtained with the conventional reduction approaches. Some of the latest developments deal with the efficient application of

*Institute of Engineering and Computational Mechanics, University of Stuttgart, Stuttgart, Germany,
{christine.nowakowski, peter.eberhard}@itm.uni-stuttgart.de

†Max Planck Institute for Dynamics of Complex Technical Systems, Magdeburg, Germany,
{benner, kuerschner}@mpi-magdeburg.mpg.de

these methods to dynamical systems of special structure, for instance, linear time invariant second order dynamical systems as they are highly relevant for the industrial application. For these systems we focus on balanced truncation model order reduction which aims at neglecting the parts of the system which are hard to control and difficult to observe. For dealing with the occurring second order systems a structure preserving modification of this reduction strategy can be applied. Pushed by promising results for large scale dynamical systems and the existence of error estimators, a joint research project supported by the Forschungsvereinigung Verbrennungskraftmaschinen (FVV) was done to investigate the applicability of modern model order reduction techniques for the reduction of elements of a combustion engine.

This paper is structured as follows: In the next section we review some basics of elastic multibody systems, including the modeling as second order linear time invariant system as well as the application of model order reduction. Section III describes the three main strategies of model reduction: conventional approaches, moment-matching with Krylov subspaces, and SVD based methods. The emphasis is drawn to the latter approach, where give more detailed information on the required numerical solution of the involved matrix equations and on the preservation of the second order structure. In Section IV a flexible crankshaft is introduced as test case from an actual industrial application, onto which the previously model reduction approaches are applied. Finally, Section V concludes.

II. FUNDAMENTALS OF ELASTIC MULTIBODY SYSTEMS

A classic multibody system (MBS) consists of rigid elements which are connected by ideal joints and coupling elements between each other and the surrounding environment. Detailed information about the concept of MBS can be found e.g. in [45]. For many engineering applications, where elastic effects can not be neglected, elastic multibody systems are used. There, the classical approach is extended by elastic bodies, [47], [48]. For systems where the elastic deformation is small compared to the rigid body motion, the floating frame of reference formulation can be used. As written in [48] it is currently the most widely used method in computer simulations of flexible multibody systems. The motion of a single flexible body or, respectively, the motion $\mathbf{r}_P(t)$ of a particular point P is separated into the nonlinear motion $\mathbf{r}_i(t)$ of the reference frame K_i and the linear elastic deformation $\mathbf{u}_P(t) = \mathbf{u}(\mathbf{R}_{iP}, t)$ with respect to the reference frame

$$\mathbf{r}_P(t) = \mathbf{r}_i(t) + \mathbf{R}_{iP} + \mathbf{u}_P(t). \quad (1)$$

The vector \mathbf{R}_{iP} that is time independent in the body fixed reference frame corresponds to the position of the point P in the undeformed state. A similar approach concerning the orientation of the coordinate system at point P leads to the rotational motion $\boldsymbol{\vartheta}_P(t) = \boldsymbol{\vartheta}_P(\mathbf{R}_{iP}, t)$ by elastic deformation. When the deformation vanishes, this kinematic formulation leads to exact modeling of the rigid body dynamics.

Using the floating frame of reference formulation, the modeling of an EMBS can be split into two parts, on the one hand modeling the multibody dynamics and on the other hand modeling the flexibility, see Figure 1. To establish the EMBS in the end of the modeling process both descriptions are combined and so the resulting equations have to be consistent.

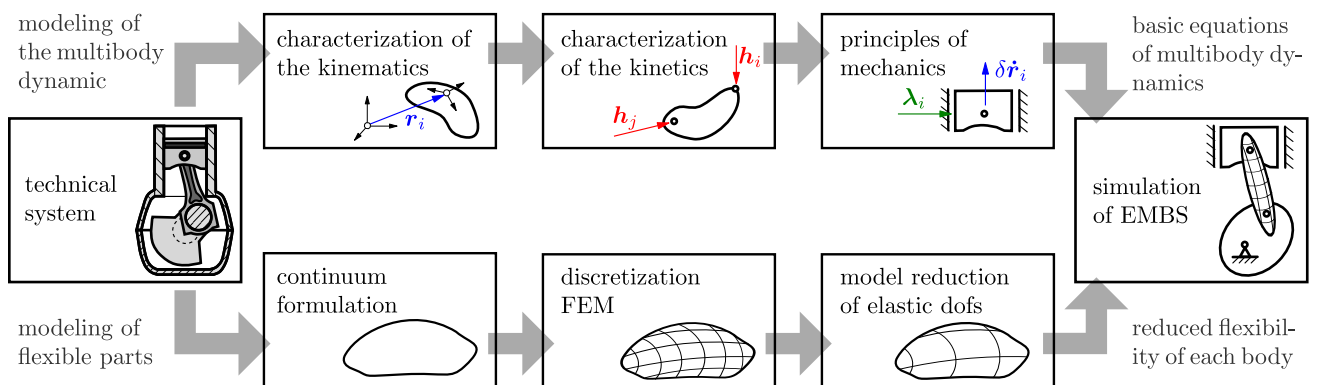


Fig. 1. Procedure of EMBS simulation.

A. Modeling the Multibody Dynamics

Based on the kinematic description, (1) the equation of motion of a single body can be derived with the help of the principles of mechanics, such as d'Alembert's or Jourdain's principle [47]. This yields the equation of motion of a single deformable body

$$\begin{bmatrix} \mathbf{M}_r^i & \mathbf{M}_{re}^i \\ \mathbf{M}_{er}^i & \mathbf{M}_e^i \end{bmatrix} \begin{bmatrix} \ddot{\mathbf{q}}_r^i \\ \ddot{\mathbf{q}}_e^i \end{bmatrix} + \begin{bmatrix} \mathbf{0} \\ \mathbf{k}_e^i \end{bmatrix} = \begin{bmatrix} \mathbf{h}_r^i \\ \mathbf{h}_e^i \end{bmatrix}, \quad (2)$$

similar to [20], [33] or [47]. Thereby, the superscript i refers to the body number. The vector of coordinates consists of the rigid body coordinates $\mathbf{q}_r \in \mathbb{R}^{N_r}$ and the elastic coordinates $\mathbf{q}_e \in \mathbb{R}^{N_e}$. The rigid multibody dynamics is described by the submatrix \mathbf{M}_r of the mass matrix and the rigid body accelerations $\ddot{\mathbf{q}}_r^T = [\mathbf{a}^T \boldsymbol{\alpha}^T]$ that contain the global translational accelerations \mathbf{a} and rotational accelerations $\boldsymbol{\alpha}$. The coupling matrices $\mathbf{M}_{er} \in \mathbb{R}^{N_e \times N_r}$ and $\mathbf{M}_{re} = \mathbf{M}_{er}^T$ take into account the interactions between the different coordinate frames. The Coriolis, centrifugal, constraint as well as the externally applied forces are summarized in the force vectors \mathbf{h}_r and \mathbf{h}_e , respectively. In general, both the mass matrix and the vector of the internal elastic forces \mathbf{k}_e are nonlinear with respect to the generalized coordinates. However, since the elastic deformations are assumed to be small the corresponding part of the equations of motions can be considered as linear with respect to the elastic degrees of freedom and thus, linear model order reduction techniques can be applied. Together with the equation of motion of each single body (2), the topology characterization and the principles of mechanics, the equation of motion of the whole elastic multibody system without kinematic loops can be written as

$$\mathbf{M}(\mathbf{q})\ddot{\mathbf{q}} + \mathbf{k}(\dot{\mathbf{q}}, \mathbf{q}, t) = \mathbf{g}(\dot{\mathbf{q}}, \mathbf{q}, t), \quad (3)$$

with the symmetric and positive definite mass matrix \mathbf{M} of the complete multibody systems, the vector of generalized gyroscopic forces \mathbf{k} , the vector of applied forces \mathbf{g} and the vector of generalized coordinates \mathbf{q} , that comprises all degrees of freedom of every body.

B. Modeling the Flexible Parts

One instrument to describe the elasticity is the linear finite element method, which is an approximation and discretization method for field problems formulated by partial differential equations [56]. In structural dynamics the displacement field of a continuum is approximated by the Ritz approach and the d'Alembert principle to get the equation of motion of a finite element model. The linear elastic deformations $\mathbf{u}(\mathbf{R}, t)$ and $\boldsymbol{\vartheta}_P(\mathbf{R}, t)$ are specified by the approach

$$\mathbf{u}(\mathbf{R}, t) = \boldsymbol{\Phi}(\mathbf{R}) \mathbf{q}_e(t), \quad \boldsymbol{\vartheta}_P(\mathbf{R}, t) = \boldsymbol{\Psi}(\mathbf{R}) \mathbf{q}_e(t), \quad (4)$$

where $\mathbf{q}_e(t)$ is referring to the nodal displacements of a finite element model and $\boldsymbol{\Phi}(\mathbf{R})$, $\boldsymbol{\Psi}(\mathbf{R})$ are the elastic shape functions, see also [33]. This results in the linear equation of motion

$$\mathbf{M}_e \ddot{\mathbf{q}}_e(t) + \mathbf{K}_e \mathbf{q}_e(t) = \mathbf{h}_e \quad (5)$$

of an elastic body as formulated in [32]. The matrices $\mathbf{M}_e, \mathbf{K}_e \in \mathbb{R}^{N_e \times N_e}$ are the mass and stiffness matrix of the flexible structure and have the following characteristics if the system is constraint sufficiently to avoid rigid body motion

$$\mathbf{M}_e = \mathbf{M}_e^T > 0, \quad \mathbf{K}_e = \mathbf{K}_e^T > 0. \quad (6)$$

The generalized surface and volume forces are summarized in the force vector \mathbf{h}_e . Additionally, for consideration of dissipative effects a damping matrix \mathbf{D}_e is usually introduced so that (5) becomes

$$\mathbf{M}_e \ddot{\mathbf{q}}_e(t) + \mathbf{D}_e \dot{\mathbf{q}}_e(t) + \mathbf{K}_e \mathbf{q}_e(t) = \mathbf{h}_e. \quad (7)$$

The damping matrix is, e.g., approximated by Rayleigh damping

$$\mathbf{D}_e = \alpha \mathbf{M}_e + \beta \mathbf{K}_e \quad (8)$$

with the factors $0 \leq \alpha, \beta$, such that obviously $\mathbf{D}_e = \mathbf{D}_e^T > 0$ holds as well. The need for high precision and complex geometries often leads to a fine spatial discretization. Mathematically the elastic body is described by a large set of linear ordinary differential equations, whose solution increases the computational effort of the simulation.

Linear model reduction is a decisive component for an efficient simulation. To get a representation used for some model reduction techniques, the forces acting on the finite element structure are described by the time dependent excitation $\mathbf{u}_e(t)$ and the input or control matrix $\mathbf{B}_e \in \mathbb{R}^{N_e \times m}$. This matrix captures the spatial distribution of the boundary and coupling conditions. Further on, the output or observation matrix $\mathbf{C}_e \in \mathbb{R}^{p \times N_e}$ is introduced for the calculation of the interesting displacements $\mathbf{y}(t)$. For this system theoretic description the equation of motion of a single elastic body can be formulated as a linear time-invariant second order multi-input multi-output (MIMO) system

$$\begin{aligned} \mathbf{M}_e \ddot{\mathbf{q}}_e(t) + \mathbf{D}_e \dot{\mathbf{q}}_e(t) + \mathbf{K}_e \mathbf{q}_e(t) &= \mathbf{B}_e \mathbf{u}_e(t), \\ \mathbf{y}(t) &= \mathbf{C}_e \mathbf{q}_e(t). \end{aligned} \quad (9)$$

C. Model Order Reduction of Elastic Degrees of Freedom

Due to increasing demands on the technical products and their simulation, the requirements on the calculation accuracy and the calculation time are often extremely high. One consequence of this trend is that the dimension of the equation of motion rises whereas the time to run the simulation should be as short as possible. Such problems particularly require an adequate model order reduction (MOR) to decrease the number of equations and keep the significant characteristics of the system. In Figure 1 the way to get a simulation of an EMBS with the help of MOR is shown.

The application of model order reduction can be described by a projection of the elastic part of the equation of motion, see [9], [19], [32], [33]. There, the large number of degrees of freedom of the flexible coordinates $\mathbf{q}_e \in \mathbb{R}^{N_e}$ are reduced by approximating \mathbf{q}_e by a representation $\tilde{\mathbf{q}}_e \in \mathbb{R}^n$ defined in a subspace \mathcal{V}_s of smaller dimension $n < N_e$

$$\mathbf{q}_e \approx \mathbf{V} \tilde{\mathbf{q}}_e. \quad (10)$$

The vector $\tilde{\mathbf{q}}_e$ is also referred to as reduced displacement vector. Let $\mathbf{V} \in \mathbb{R}^{N_e \times n}$ be the projection matrix representing the subspace \mathcal{V} , i.e. it has the basis vectors as columns. Introducing this relation into the FE equation of motion (9) leads to an over-determined system and leaves a residuum since the exact solution \mathbf{q}_e is in general not an element of the subspace. To obtain a unique solution one imposes that the residual is orthogonal to a second subspace \mathcal{W}_s represented by another projection matrix $\mathbf{W} \in \mathbb{R}^{N_e \times n}$. This orthogonality condition is often called Petrov-Galerkin condition [2], [26], [42] and results in the reduced FE equations

$$\begin{aligned} \tilde{\mathbf{M}}_e \ddot{\tilde{\mathbf{q}}}_e + \tilde{\mathbf{D}}_e \dot{\tilde{\mathbf{q}}}_e + \tilde{\mathbf{K}}_e \tilde{\mathbf{q}}_e &= \tilde{\mathbf{B}}_e \mathbf{u}_e, \\ \tilde{\mathbf{y}} &= \tilde{\mathbf{C}}_e \tilde{\mathbf{q}}_e, \end{aligned} \quad (11)$$

with the reduced mass matrix $\tilde{\mathbf{M}}_e := \mathbf{W}^T \mathbf{M}_e \mathbf{V}$, damping matrix $\tilde{\mathbf{D}}_e := \mathbf{W}^T \mathbf{D}_e \mathbf{V}$, stiffness matrix $\tilde{\mathbf{K}}_e := \mathbf{W}^T \mathbf{K}_e \mathbf{V} \in \mathbb{R}^{n \times n}$, and the reduced input and output matrices $\tilde{\mathbf{B}}_e := \mathbf{W}^T \mathbf{B}_e \in \mathbb{R}^{n \times m}$, $\tilde{\mathbf{C}}_e := \mathbf{C}_e \mathbf{V} \in \mathbb{R}^{m \times n}$. The projection is called orthogonal if the subspaces are identical, i.e. $\mathbf{V} = \mathbf{W}$, and oblique otherwise. This procedure leads to the reduced equations of motion of a single flexible body

$$\begin{bmatrix} \mathbf{M}_r & \mathbf{M}_{er}^T \mathbf{V} \\ \mathbf{W}^T \mathbf{M}_{er} & \tilde{\mathbf{M}}_e \end{bmatrix} \begin{bmatrix} \dot{\tilde{\mathbf{q}}}_r \\ \dot{\tilde{\mathbf{q}}}_e \end{bmatrix} + \begin{bmatrix} \mathbf{0} \\ \tilde{\mathbf{K}}_e \tilde{\mathbf{q}}_e + \tilde{\mathbf{D}}_e \dot{\tilde{\mathbf{q}}}_e \end{bmatrix} = \begin{bmatrix} \mathbf{h}_r \\ \tilde{\mathbf{h}}_e \end{bmatrix}, \quad (12)$$

where the reduced forces and moments are defined as $\tilde{\mathbf{h}}_e := \mathbf{W}^T \mathbf{h}_e \in \mathbb{R}^n$. In engineering applications it can be helpful to preserve the structural properties (6). In such cases an orthogonal projection has to be performed, e.g. by assuming $\mathbf{C}_e = \mathbf{B}_e^T$. The differences of the reduction techniques mentioned above are the principles, which establish how the projection matrices are generated.

III. MODEL REDUCTION TECHNIQUES

In industrial settings and software environments methods based on modal reduction, condensation and component mode synthesis (CMS) are still the state of the art methods. Modern reduction techniques like moment-matching with Krylov subspace based method or reduction approaches based on the singular value decompositions (SVD), for example balanced truncation, were introduced in the last decades. These methods use different ways to approximate

the input to output mapping of the dynamical system describing the underlying physical or technical process. For the application in the simulation of elastic bodies, there are mainly three classes of model reduction techniques:

- classical reduction techniques such as modal reduction, condensation and component mode synthesis,
- SVD-based approximation methods using Gramian matrices, or
- techniques based on moment-matching via Krylov subspaces.

Each of the reduction techniques mentioned above has its specific advantages and disadvantages. The following criteria are of special interest for the user: computability for large scale systems, stability preservation, quality of the reduced order model, knowledge about the error induced through the approximation. For the particular application discussed here, the preservation of the second order structure, an emphasis onto a certain frequency range, and the possibility to automate the reduction process are also of relevance.

A. State of the Art Reduction Techniques

In structural mechanics and elastic multibody dynamics the most frequently used model order reductions are techniques based on modal reduction and substructuring. Modal reduction relies on a transformation of the geometric coordinates of the FE model into a system of modal coordinates as given in [31]. The nodal displacement vector is approximated by a linear combination of r modes

$$\mathbf{q}_e = \sum_{i=1}^r \phi_i e^{\lambda_i t} = \Phi \mathbf{q}_{\text{modal}}, \quad (13)$$

where ϕ_i are, for example, dominant eigenvectors of the free (free-free normal modes) or a bounded (fixed-interface normal modes) body. A suitable normalization of the modes requires

$$\phi_i M_e \phi_j = \delta_{ij}. \quad (14)$$

a) Condensation (Guyan reduction): Static condensation is done by substructuring the nodal displacement vector into internal or slave \mathbf{q}_i and external or master \mathbf{q}_e degrees of freedom, see [35] or [30]. As in [15], [16], the external coordinates are redundant and the internal ones are kept as the remaining node displacement coordinates.

b) Mixed static modal (Craig-Bampton): The combination of condensation and modal reduction of the internal structure by superposition results in an approximation of the internal degrees of freedom by

$$\mathbf{q}_s = -\mathbf{K}_{ei} \mathbf{K}_{ii}^{-1} \mathbf{q}_m + \Phi_{\text{internal}} \mathbf{q}_{\text{intmodal}} \quad (15)$$

with parts of the stiffness matrix \mathbf{K}_{ei} and \mathbf{K}_{ii} and the Craig-Bampton [16] projection matrix becomes

$$\mathbf{V}_{\text{CMS}} = \begin{bmatrix} \mathbf{I} & \mathbf{0} \\ -\mathbf{K}_{ei} \mathbf{K}_{ii}^{-1} & \Phi_{\text{internal}} \end{bmatrix}. \quad (16)$$

The convergence of modal reduction can be slow, e.g. because the spatial distribution of loads is not mandatory considered. In addition, no information about the error introduced by model reduction can be gained and a tuning of the reduced model for certain frequency ranges is not possible. Modal reduction can be improved by extending the projection space with other modes. However, often the selection of the dominant eigenmodes requires a lot of experience by the engineer, so that these method can be hardly automated.

B. Methods based on Krylov subspaces

1) Basic Idea: In these reduction techniques the frequency response is taken as a characteristic quantity to describe the original system. The basic idea is to approximate the transfer function matrix

$$\mathbf{H}(s) = \mathbf{C}_e (s^2 \mathbf{M}_e + s \mathbf{D}_e + \mathbf{K}_e)^{-1} \mathbf{B}_e, \quad s \in \mathbb{C} \quad (17)$$

by matching several values and derivatives at different points which are usually called expansion or interpolation points, respectively, or simply shifts [26], [32].

For this purpose, the transfer function matrix is expanded into a power series, whose coefficients $\mathbf{T}_j^{\sigma_k}$ are called moments of order j with respect to an expansion point $\sigma_k \in \mathbb{C}$ of the transfer function. To match several values and derivatives, it is required that the moments to these specific expansion points of the original and the reduced

transfer function matrix match. This is realized in [26] for systems of first order by using the rational Krylov approach by projecting the system onto rational Krylov subspaces. For second order systems one uses second order Krylov subspaces [4], [44] which are for a given shift σ_k given by

$$\begin{aligned} \mathcal{G}^r(\bar{\mathbf{P}}_k, \bar{\mathbf{Q}}_k; \mathbf{S}_k) &:= \text{span}\{\mathbf{R}_0, \mathbf{R}_1, \mathbf{R}_2, \dots, \mathbf{R}_{r-1}\}, \\ \mathbf{R}_j &:= p_j(\bar{\mathbf{P}}_k, \bar{\mathbf{Q}}_k)\mathbf{S}_k. \end{aligned} \quad (18)$$

There, using

$$\mathbf{L}_k := \sigma_k^2 \mathbf{M}_e + \sigma_k \mathbf{D}_e + \mathbf{K}_e, \quad \mathbf{N}_k := 2\sigma_k \mathbf{M}_e + \mathbf{D}_e, \quad (19)$$

the defining matrices are given by

$$\bar{\mathbf{P}}_k := -\mathbf{L}_k^{-1} \mathbf{N}_k, \quad \bar{\mathbf{Q}}_k := -\mathbf{L}_k^{-1} \mathbf{M}_e, \quad \text{and} \quad \mathbf{S}_k := \mathbf{L}_k^{-1} \mathbf{B}_e. \quad (20)$$

Furthermore, $p_j(\alpha, \beta)$ is a bivariate polynomial following the recursion

$$p_j(\alpha, \beta) = \alpha p_{j-1}(\alpha, \beta) + \beta p_{j-2}(\alpha, \beta) \quad (21)$$

with $p_0(\alpha, \beta) \equiv 1$ and $p_1(\alpha, \beta) = \alpha$. The second order Krylov subspace can be generated with a second order Arnoldi method (SOAR) [5]. Using different expansion points σ_k and matching moments of order J_k , the rational second order Krylov subspace is constructed by concatenating all the second order Krylov subspaces associated to one shift σ_k

$$\bigcup_k \mathcal{G}^{J_k}(\bar{\mathbf{P}}_k, \bar{\mathbf{Q}}_k; \mathbf{S}_k) \subseteq \mathcal{V}_s = \text{colsp}(\mathbf{V}). \quad (22)$$

Additionally, one can define another rational second order Krylov subspace for the left transformation

$$\bigcup_k \mathcal{G}^{F_k}(-\mathbf{L}_k^{-H} \mathbf{N}_k^H, -\mathbf{L}_k^{-H} \mathbf{M}_e^T; \mathbf{L}_k^{-H} \mathbf{C}_e) \subseteq \mathcal{W}_s = \text{colsp}(\mathbf{W}), \quad (23)$$

where the orders F_k of the moments do not have to coincide with J_k . Both spaces can be constructed simultaneously using a two-sided second order Arnoldi method [44].

2) *Advantages and Disadvantages:* The fact that Krylov subspace based reduction methods are iterative methods and can be applied to large scale models represents their decisive advantage. The performance of Krylov subspace based reduction methods clearly depends on the choice of expansion points, leading to developments for automated shift selections in recent years. In addition, error estimation is nowadays possible, see [22], which means that the user has much more control over the validation of his simulation. However, the method lacks flexibility with respect to systems with many inputs or outputs, since with an increasing order of the moments, mJ_k new basis vectors are added to the Krylov subspace for each shift σ_k . This can be circumvented by constructing the Krylov subspaces with the help of tangential interpolation [23].

C. SVD based Reduction Techniques

1) *Basic Idea for Systems of First Order:* Another large group of reduction techniques are methods based on a singular value decomposition (SVD) or Gramian matrices. The basic motivation for this reduction is the energy interpretation of the input output map of the system. There, the governing question is: which states of the system require the most excitation energy and produce the least output energy? These states would yield no important contributions to the system dynamics and can be neglected. This identification and truncation is carried out in balanced truncation model order reduction [37], [2] which was intrinsically designed for standard state space systems of the form

$$\begin{aligned} \dot{\mathbf{x}} &= \mathbf{A}\mathbf{x} + \mathbf{B}\mathbf{u}, \\ \mathbf{y} &= \mathbf{C}\mathbf{x}. \end{aligned} \quad (24)$$

Here we present the basic principles of balanced truncation for generalized first order systems

$$\begin{aligned} \mathbf{E}\dot{\mathbf{x}} &= \mathbf{A}\mathbf{x} + \mathbf{B}\mathbf{u}, \\ \mathbf{y} &= \mathbf{C}\mathbf{x}, \end{aligned} \quad (25)$$

which are more relevant for our purposes and for which balanced truncation can be modified appropriately in a straightforward way as it was shown in, e.g., [8], [13], [43]. The controllability and observability Gramian matrices, P and Q , of (25) are strongly related to the above energy interpretation. For an asymptotically stable system they are the unique solutions of the generalized Lyapunov equations

$$APE^T + EPA^T = -BB^T, \quad (26)$$

$$A^TQE + E^TQA = -C^TC. \quad (27)$$

The Gramian matrices P , Q are symmetric matrices which are also positive definite if the system in (25) is in addition controllable and observable which we assume for the remainder. Hence there exist Cholesky factorizations $P = RR^T$, $Q = SS^T$. The eigenvalues of P or Q are a measure of how strongly the states can be controlled or observed. Moreover, the eigenvalues of the product PE^TQE give a combined measurement of how good states can be controlled and observed. Note that the eigenvalue relation $PE^TQE\mathbf{x} = \lambda\mathbf{x}$ is equivalent to $R^TE^TSS^TER\mathbf{y} = \lambda\mathbf{y}$ with $\mathbf{y} := R^{-1}\mathbf{x}$ and hence, the square roots of the eigenvalues are the singular values of S^TER which are system invariants and referred to as Hankel singular values (HSV)

$$\sigma_j := \sqrt{\lambda_j(PE^TQE)}. \quad (28)$$

Note that the positive definiteness of the Gramian matrices is actually not necessary, since the above can also be carried out by using Cholesky-like, or low-rank, factorizations $P \approx \tilde{R}\tilde{R}^T$, $Q \approx \tilde{S}\tilde{S}^T$, as it is done in a large-scale setting anyway. We investigate the numerical computation of such low-rank factors in Section III-C2.

It is the goal of this reduction to determine those state components which have no or little effect on the energy transfer. These state components can be identified by the associated small Hankel singular values. This can be achieved by applying a balancing transformation to (25) such that $P = Q = \Sigma = \text{diag}(\sigma_1, \dots, \sigma_n)$ from which the small, to be neglected, HSVs can be read off easily. The complete procedure of balanced truncation including these transformations is schematically given in Algorithm 1.

Algorithm 1 Balanced truncation for generalized state-space systems

Input: System matrices E , A , B , C defining the dynamical system (25), truncation tolerance ε_{BT}

Output: Matrices \tilde{E} , \tilde{A} , \tilde{B} , \tilde{C} of reduced system

- 1: Compute Cholesky factors R , S of the solutions of (26), (27).
- 2: Compute and partition a (thin) singular value decomposition

$$XSY^T = [X_1 \ X_2] \begin{bmatrix} \Sigma_1 & 0 \\ 0 & \Sigma_2 \end{bmatrix} [Y_1 \ Y_2]^T = S^TER,$$

where (29) can be used to define $\Sigma_1 := \Sigma(1:n, 1:n)$ and the other adequately sized blocks.

- 3: Construct transformation matrices V and W

$$V := RY_1\Sigma_1^{-\frac{1}{2}}, \quad W := SX_1\Sigma_1^{-\frac{1}{2}}.$$

- 4: Generate reduced order realization

$$\tilde{E} := W^TEV, \quad \tilde{A} := W^TAV, \quad \tilde{B} := W^TB, \quad \tilde{C} := CV.$$

Let σ_{n+1} denote the largest neglected HSV, and H , \tilde{H} are the transfer functions of the original and reduced first order system. Then the error bound

$$\|H - \tilde{H}\|_{\mathcal{H}_\infty} \leq 2 \sum_{i=n+1}^N \sigma_i \quad (29)$$

holds which can be used to adaptively determine n , i.e., the reduced system's order, by truncating the SVD in step 2 of Algorithm 1 as the sum in (29) falls below a tolerance ε_{BT} . Furthermore in [1] the value

$$\frac{\sigma_{n+1}}{\sigma_1} < \tau \quad (30)$$

assigns the error of the approximation for $\|\mathbf{y} - \mathbf{y}_{red}\|$ over the entire frequency range. It is recommended to set τ in relation to the machine precision, typically $\tau = \sqrt{\epsilon}$. Note that $\tilde{\mathbf{E}}$ is always the identity matrix \mathbf{I}_n . The steps requiring the most computational work are the solution of the generalized Lyapunov equations in step 1 and the computation of the SVD in step 2. In the next section we show an algorithm that computes approximations to \mathbf{P} , \mathbf{Q} in an efficient way via low-rank versions of \mathbf{R} , \mathbf{S} which in turn will also render the SVD computation numerically inexpensive.

2) *Solving the Lyapunov Equations*: If the size N of \mathbf{A} and \mathbf{E} is small or moderately large, methods based on the Schur decomposition can be used to solve (26) and (27). The most prominent of such methods for this case are the Bartels-Stewart algorithm [7] and Hammerling's method [27]. The alternating directions implicit (ADI) method [54], [55] is another method of iterative nature for solving Lyapunov equations. Since in our application N will be large, the usage of these methods is not feasible for solving the corresponding generalized Lyapunov equations due to their cubic complexity. However, practical observations as well as recent theoretical investigations [50], [25] show that \mathbf{P} , \mathbf{Q} , and thus their Cholesky factors \mathbf{R} , \mathbf{S} , have a small numerical rank, i.e., their singular values decay quite rapidly towards zero. Hence, they can be approximated by low-rank Cholesky factors (LRCFs) $\tilde{\mathbf{R}} \in \mathbb{R}^{N_e \times r_1}$, $\tilde{\mathbf{S}} \in \mathbb{R}^{N_e \times r_2}$ with $r_1, r_2 \ll N_e$ and such that $\tilde{\mathbf{R}}\tilde{\mathbf{R}}^T \approx \mathbf{P}$, $\tilde{\mathbf{S}}\tilde{\mathbf{S}}^T \approx \mathbf{Q}$.

This is the foundation for the low-rank-Cholesky-factor ADI (LRCF-ADI) method [40], [34], [11] which reformulates the ADI method to produce LRCFs. The generalized LRCF-ADI (G-LRCF-ADI) is a version of LRCF-ADI capable to solve generalized Lyapunov equations [43], [12], [8] and is illustrated in Algorithm 2.

Note that there is another class of methods using Krylov subspaces for computing low-rank factors of the solution, see e.g. [49]. In contrast to ADI based method, to apply these methods the system has to be dissipative, i.e., $\mathbf{A}\mathbf{E}^T + \mathbf{E}\mathbf{A}^T$ has to be negative definite, which is too restrictive for our purposes. Later on we briefly return to this issue.

Algorithm 2 Generalized low-rank Cholesky factor ADI iteration (G-LRCF-ADI)

Input: \mathbf{E} , \mathbf{A} and \mathbf{B} , or \mathbf{C} as in (26), (27) and shift parameters $\{\mu_1, \dots, \mu_{j_{max}}\} \subset \mathbb{C}_-$.

Output: $\mathbf{Z} = \mathbf{Z}_{j_{max}} \in \mathbb{C}^{n \times t_{j_{max}}}$, such that $\mathbf{Z}\mathbf{Z}^H \approx \mathbf{P}$, \mathbf{Q} in (26),(27), respectively.

```

1: if right hand side given is  $\mathbf{C}$  then
2:   Transpose  $\mathbf{A}$ ,  $\mathbf{E}$  and set  $\mathbf{B} = \mathbf{C}^T$ .
3: end if
4: for  $j = 1, 2, \dots, j_{max}$  do
5:   if  $j = 1$  then
6:      $\mathbf{V}_1 = \sqrt{-2 \operatorname{Re}(\mu_1)}(\mathbf{A} + \mu_1 \mathbf{E})^{-1} \mathbf{B}$ 
7:      $\mathbf{Z}_1 = \mathbf{V}_1$ 
8:   else
9:      $\mathbf{V}_j = \sqrt{\operatorname{Re}(\mu_j) / \operatorname{Re}(\mu_{j-1})}(\mathbf{V}_{j-1} - (\mu_j + \overline{\mu_{j-1}})(\mathbf{A} + \mu_j \mathbf{E})^{-1} \mathbf{V}_{j-1})$ 
10:     $\mathbf{Z}_j = [\mathbf{Z}_{j-1}, \mathbf{V}_j]$ 
11:   end if
12: end for

```

The set of shift parameters $\{\mu_1, \dots, \mu_{j_{max}}\}$ required in Algorithm 2 is closed with respect to complex conjugation and steers the convergence of the iteration. The optimal set of shift parameters can be related to a rational minmax problem [55] which involves all eigenvalues of the generalized eigenvalue problem $\mathbf{A}\mathbf{x} = \lambda \mathbf{E}\mathbf{x}$, $\mathbf{0} \neq \mathbf{x} \in \mathbb{C}^N$. Since for large matrices the complete spectrum $\Lambda(\mathbf{A}, \mathbf{E})$ cannot be computed efficiently, a common approach uses a small number of approximate eigenvalues which are obtained from $k_+ \ll N$ Ritz values of $\mathbf{E}^{-1}\mathbf{A}$ and the inverses of $k_- \ll N$ Ritz values of $\mathbf{A}^{-1}\mathbf{E}$, where both subsets can be computed with an Arnoldi process. The shift parameters obtained by solving the rational minmax problem approximately using these Ritz values are often called heuristic, or Penzl shifts [40].

Since the systems discussed here represent elastic bodies, it is highly likely that \mathbf{A} , \mathbf{E} have complex eigenvalues. Consequently, the obtained Ritz values and thus also the shift parameters are complex. This will inevitably introduce complex arithmetic computations in Algorithm 2 and the final LRCFs $\tilde{\mathbf{R}}$, $\tilde{\mathbf{S}}$ are then complex matrices. Consequently, the matrix $\tilde{\mathbf{S}}^T \mathbf{E} \tilde{\mathbf{R}}$ used in Algorithm 1 is complex resulting in a complex reduced order model. Since

this is undesirable and arithmetic operations with complex numbers are more expensive than with real ones, an algorithm using only real arithmetics and producing real LRCFs is preferred. In [11, Algorithm 4] it is shown how the LRCF-ADI method can be rewritten to achieve this goal. However, another approach given in [10] generates real low-rank factors as well, but appears to be more efficient in term of the computational complexity although temporarily still complex arithmetic operations are employed. In the remainder we assume we have generated real LRCFs using the latter approach.

The algorithm can be terminated after a maximum number j_{\max} of iterations is reached, or if the normalized residual of the current approximation is of sufficient accuracy, e.g. if the norm of the residual falls below a given tolerance. Alternatively, one can monitor the relative change of the current LRCF approximation in the Frobenius norm. See [43], [11] for more information on stopping criteria for the ADI method.

Solving the linear systems in steps 6 and 9 are the most expensive operations in the algorithm and we assume that we are able to employ sparse direct solvers [18], e.g. a sparse LU factorisation, for their solution. Note that instead of computing $\tilde{\mathbf{R}}$, $\tilde{\mathbf{S}}$ separately by two runs of Algorithm 2, a simultaneous computation is also possible by, for instance, reusing the LU factorization $\mathbf{LU} = \mathbf{A} + \mu_j \mathbf{E}$ in each step for the solution of the adjoint linear system.

Since in each iteration m columns (the number of columns in \mathbf{B} (or \mathbf{C}^T)) are added to the current LRCF iterate \mathbf{Z} , we assume that $m \ll N_e$ such that the number of columns in \mathbf{Z} does not grow too fast.

After termination of Algorithm 2, the LRCFs $\tilde{\mathbf{R}}$, $\tilde{\mathbf{S}}$ will usually have $r_1, r_2 \ll N_e$ columns and hence, the matrix $\tilde{\mathbf{S}}^T \mathbf{E} \tilde{\mathbf{R}} \in \mathbb{R}^{r_1 \times r_2}$ is small such that the computation of the SVD in step 2 of Algorithm 1 is inexpensive.

3) *Treatment of Second Order Systems:* To apply the balanced truncation process to second order systems (9), one usually chooses an equivalent first order system. This reformulation into a system of the form (25) is closely related to a transformation of the associated quadratic eigenvalue problem $(\lambda^2 \mathbf{M}_e + \lambda \mathbf{D}_e + \mathbf{K}_e) \mathbf{x} = \mathbf{0}$, $\mathbf{x} \neq \mathbf{0}$, into a generalized linear eigenvalue problem $(\lambda \mathbf{E} - \mathbf{A}) \mathbf{z} = \mathbf{0}$, $\mathbf{z} = [\mathbf{x}^T, \lambda \mathbf{x}^T]^T \neq \mathbf{0}$. Therefore, the reformulation is sometimes also called linearization of the λ -matrix.

There are several linearizations possible [51], but since for the application discussed here, mass, damping and stiffness matrices of (9) are assumed to be symmetric, and it holds $\mathbf{B}_e = \mathbf{C}_e^T$, it is beneficial to take

$$\mathbf{x} := \begin{bmatrix} \mathbf{q}_e \\ \dot{\mathbf{q}}_e \end{bmatrix}, \quad \mathbf{E} := \begin{bmatrix} \mathbf{D}_e & \mathbf{M}_e \\ \mathbf{M}_e & \mathbf{0} \end{bmatrix}, \quad \mathbf{A} := \begin{bmatrix} -\mathbf{K}_e & \mathbf{0} \\ \mathbf{0} & \mathbf{M}_e \end{bmatrix} \in \mathbb{R}^{2N_e \times 2N_e}, \quad \mathbf{B} := \begin{bmatrix} \mathbf{B}_e \\ \mathbf{0} \end{bmatrix} = \mathbf{C}^T \in \mathbb{R}^{2N_e \times m}. \quad (31)$$

This has the advantage that \mathbf{E} and \mathbf{A} are symmetric matrices, $\mathbf{B} = \mathbf{C}^T$, such that both generalized Lyapunov equations (26) and (27) coincide which implies $\mathbf{P} \equiv \mathbf{Q}$ and hence, $\mathbf{R} \equiv \mathbf{S} =: \mathbf{Z}$. Consequently, only the solution, respectively its (low-rank) Cholesky factor, of one single Lyapunov equation is sufficient to carry out balanced truncation which relaxes the computational effort drastically.

Note that the assumptions on the system matrices to obtain these properties are rather strong. Even the case $\mathbf{B}_e \neq \mathbf{C}_e^T$ will lead to different Lyapunov equations and hence to different controllability and observability Gramian matrices.

As shown in [13], a generalized system with matrices of the form (31) can only be dissipative if $\mathbf{M}_e = \mathbf{K}_e$. This is by far a too restrictive assumption on realistic systems and in particular not fulfilled in our case, applying projection based Krylov subspace methods [49] for solving the generalized Lyapunov equations is not feasible. This short discussion serves as an extra motivation for the application of low-rank ADI based methods for this purpose.

Although a straightforward application of Algorithm 1 including one run of the G-LRCF-ADI method (Algorithm 2) with the matrices \mathbf{E} , \mathbf{A} , \mathbf{B} defining the first order system (25) is possible, it has two severe drawbacks. At first, Algorithm 1 will produce transformation matrices \mathbf{V} , $\mathbf{W} \in \mathbb{R}^{2N_e \times r}$ that are only applicable to the first order system, resulting in a reduced system of first order and losing the second order structure. Secondly, working with the first order matrices of dimension $2N_e \times 2N_e$ within G-LRCF-ADI introduces a huge amount of additional computational work. There, it is desired to work with the original $N_e \times N_e$ matrices of the second order systems. In the sequel we discuss both issues, beginning with the latter one.

a) *Efficient Computation of LRCFs for Systems of Second Order:* The main operations in the G-LRCF-ADI method are solving linear systems of the form $(\mathbf{A} + \mu \mathbf{E}) \mathbf{f} = \mathbf{g}$ and $(\mathbf{A} + \mu \mathbf{E}) \mathbf{f} = \mathbf{E} \mathbf{g}$ for \mathbf{f} , $\mathbf{g} \in \mathbb{R}^{2N \times m}$. As described above, due to the symmetry of \mathbf{A} and \mathbf{E} the transposed linear systems are not required. To rewrite these steps such that the original matrices of (9) are used, we split the sought solution \mathbf{f} of the linear systems and the

corresponding right hand side \mathbf{g} into upper and lower blocks

$$\mathbf{f} = \begin{bmatrix} \mathbf{f}^{(1)} \\ \mathbf{f}^{(2)} \end{bmatrix}, \quad \mathbf{g} = \begin{bmatrix} \mathbf{g}^{(1)} \\ \mathbf{g}^{(2)} \end{bmatrix}, \quad \mathbf{f}^{(i)}, \mathbf{g}^{(i)} \in \mathbb{R}^{N_e \times m}, \quad i = 1, 2. \quad (32)$$

In the initial step of Algorithm 2 one has to solve $(\mathbf{A} + \mu_1 \mathbf{E})\mathbf{f} = \mathbf{g}$ for \mathbf{f} . Exploiting the structure of \mathbf{A} , \mathbf{E} leads to

$$\begin{bmatrix} -\mathbf{K}_e + \mu_1 \mathbf{D}_e & \mu_1 \mathbf{M}_e \\ \mu_1 \mathbf{M}_e & \mathbf{M}_e \end{bmatrix} \begin{bmatrix} \mathbf{f}^{(1)} \\ \mathbf{f}^{(2)} \end{bmatrix} = \begin{bmatrix} \mathbf{g}^{(1)} \\ \mathbf{g}^{(2)} \end{bmatrix} = \mathbf{B} = \begin{bmatrix} \mathbf{B}_e \\ \mathbf{0} \end{bmatrix}, \quad (33)$$

or equivalently,

$$\begin{aligned} -\mathbf{K}_e \mathbf{f}^{(1)} + \mu_1 \mathbf{D}_e \mathbf{f}^{(1)} + \mu_1 \mathbf{M}_e \mathbf{f}^{(2)} &= \mathbf{B}_e, \\ \mu_1 \mathbf{M}_e \mathbf{f}^{(1)} + \mathbf{M}_e \mathbf{f}^{(2)} &= \mathbf{0}. \end{aligned} \quad (34)$$

From the lower equation in (34) and the invertibility of \mathbf{M}_e it follows that $\mathbf{f}^{(2)} = -\mu_1 \mathbf{f}^{(1)}$ which, after inserting into the upper equation, gives

$$(\mu_1^2 \mathbf{M}_e - \mu_1 \mathbf{D}_e + \mathbf{K}_e) \mathbf{f}^{(1)} = -\mathbf{B}_e. \quad (35)$$

Similar manipulations can be done for the increment in the j th iteration, where $(\mathbf{A} + \mu_j \mathbf{E})\mathbf{f} = \mathbf{E}\mathbf{g}$ is solved for \mathbf{f} , which is equivalent to

$$\begin{bmatrix} -\mathbf{K}_e + \mu_j \mathbf{D}_e & \mu_j \mathbf{M}_e \\ \mu_j \mathbf{M}_e & \mathbf{M}_e \end{bmatrix} \begin{bmatrix} \mathbf{f}^{(1)} \\ \mathbf{f}^{(2)} \end{bmatrix} = \begin{bmatrix} \mathbf{D}_e \mathbf{g}^{(1)} + \mathbf{M}_e \mathbf{g}^{(2)} \\ \mathbf{M}_e \mathbf{g}^{(1)} \end{bmatrix}. \quad (36)$$

Thus, $\mathbf{f}^{(2)} = \mathbf{g}^{(1)} - \mu_j \mathbf{f}^{(1)}$ which eventually yields

$$(\mu_j^2 \mathbf{M}_e - \mu_j \mathbf{D}_e + \mathbf{K}_e) \mathbf{f}^{(1)} = (\mu_j \mathbf{M}_e - \mathbf{D}_e) \mathbf{g}^{(1)} - \mathbf{M}_e \mathbf{g}^{(2)}. \quad (37)$$

Including these equations into G-LRCF-ADI leads to the second-order LRCF-ADI (SO-LRCF-ADI) shown in Algorithm 3. For using only operations with the original $N_e \times N_e$ matrices one has to solve linear systems involving quadratic matrix polynomials of the form $\mu_j^2 \mathbf{M}_e - \mu_j \mathbf{D}_e + \mathbf{K}_e$. For avoiding additional numerical problems it is often wise to restrict the absolute values of the shift parameters to circumvent that μ_j^2 does not dominate over the norm of the matrices.

We want to emphasise, that the single steps of Algorithm 3 crucially depend on the selected equivalent first order system. Choosing another linearization will ultimately lead to another reformulation of G-LRCF-ADI, for instance, as in [43], [12], [13].

In the presence of complex shift parameters, it is again possible to rewrite Algorithm 3 into a real form along the lines of [11, Algorithm 4] or to apply the strategy proposed in [10] in order to generate real LRCFs.

b) Structure Preserving Balanced Truncation for Second Order Systems.: In [41], [57], [14], [36] modifications of balanced truncation for the construction of reduced systems of second order are presented. The main idea there is to partition the LRCFs $\tilde{\mathbf{R}}$, $\tilde{\mathbf{S}}$ of \mathbf{P} , \mathbf{Q} accordingly with respect to the structure of the first order system matrices

$$\tilde{\mathbf{R}} = \begin{bmatrix} \tilde{\mathbf{R}}_p \\ \tilde{\mathbf{R}}_v \end{bmatrix}, \quad \tilde{\mathbf{S}} = \begin{bmatrix} \tilde{\mathbf{S}}_p \\ \tilde{\mathbf{S}}_v \end{bmatrix}, \quad \tilde{\mathbf{R}}_p, \tilde{\mathbf{R}}_v, \tilde{\mathbf{S}}_p, \tilde{\mathbf{S}}_v \in \mathbb{R}^{N_e \times r_{1,2}}, \quad (38)$$

where the subscripts p , v refer to the position and velocity component in the generalized state space vector \mathbf{x} of (25). Compatibly partitioning the (approximate) Gramian matrices

$$\mathbf{P} = \begin{bmatrix} \mathbf{P}_p & \mathbf{P}_o \\ \mathbf{P}_o & \mathbf{P}_v \end{bmatrix} \approx \begin{bmatrix} \tilde{\mathbf{R}}_p \\ \tilde{\mathbf{R}}_v \end{bmatrix} \begin{bmatrix} \tilde{\mathbf{R}}_p \\ \tilde{\mathbf{R}}_v \end{bmatrix}^T = \tilde{\mathbf{R}} \tilde{\mathbf{R}}^T, \quad (39)$$

$$\mathbf{Q} = \begin{bmatrix} \mathbf{Q}_p & \mathbf{Q}_o \\ \mathbf{Q}_o & \mathbf{Q}_v \end{bmatrix} \approx \begin{bmatrix} \tilde{\mathbf{S}}_p \\ \tilde{\mathbf{S}}_v \end{bmatrix} \begin{bmatrix} \tilde{\mathbf{S}}_p \\ \tilde{\mathbf{S}}_v \end{bmatrix}^T = \tilde{\mathbf{S}} \tilde{\mathbf{S}}^T \quad (40)$$

reveals the second order Gramian matrices which are the diagonal blocks. According to [41], \mathbf{P}_p , \mathbf{Q}_p are referred to as position controllability and, respectively, observability Gramian matrices. Similarly, \mathbf{P}_v , \mathbf{Q}_v are called velocity

Algorithm 3 (Second-Order Low-rank Cholesky factor ADI iteration (SO-LRCF-ADI))

Input: M_e, D_e, K_e, B_e defining (9) and shift parameters $\{\mu_1, \dots, \mu_{j_{\max}}\}$.

Output: $\tilde{Z} \in \mathbb{C}^{2N \times tj_{\max}}$, such that $\tilde{Z}\tilde{Z}^H \approx P = Q$ in (26), (27).

- 1: **for** $j = 1, 2, \dots, j_{\max}$ **do**
- 2: **if** $j = 1$ **then**
- 3: Solve $(\mu_1^2 M_e - \mu_1 D_e + K_e) \hat{V}^{(1)} = -B_e$ for $\hat{V}^{(1)}$, set $\hat{V}^{(2)} = -\mu_1 \hat{V}^{(1)}$.
- 4: $V_1 = \sqrt{-2 \operatorname{Re}(\mu_1)} \begin{bmatrix} \hat{V}^{(1)} \\ \hat{V}^{(2)} \end{bmatrix}$.
- 5: $\tilde{Z} = V_1$.
- 6: **else**
- 7: Solve $(\mu_j^2 M_e - \mu_j D_e + K_e) \hat{V}^{(1)} = (\mu_j M_e - D_e) V_{j-1}^{(1)} - M_e V_{j-1}^{(2)}$ for $\hat{V}^{(1)}$, set $\hat{V}^{(2)} = V_{j-1}^{(1)} - \mu_j \hat{V}^{(1)}$.
- 8: $V_j = \sqrt{\frac{\operatorname{Re}(\mu_j)}{\operatorname{Re}(\mu_{j-1})}} \left(V_{j-1} - (\mu_j + \overline{\mu_{j-1}}) \begin{bmatrix} \hat{V}^{(1)} \\ \hat{V}^{(2)} \end{bmatrix} \right)$.
- 9: $\tilde{Z} = [\tilde{Z}, V_j]$.
- 10: **end if**
- 11: **end for**

controllability and observability Gramian matrices. By simultaneously diagonalizing one controllability and one observability second order Gramian matrix we arrive at a total of four different ways to carry out balancing and thus also balanced truncation. For example, choosing (P_p, Q_p) leads to a position-position balanced reduced order model. Likewise, one could take (P_p, Q_v) for position-velocity, (P_v, Q_p) for velocity-position, and (P_v, Q_v) for velocity-velocity balanced truncation. Table I summarizes the associated transformations and the involved SVDs of all possibilities. The entries, e.g., of the block $\Sigma_{\nu\xi}$ are referred to as position-position, velocity-velocity, velocity-position, or position-velocity singular values, depending on the choice of $\nu, \xi \in \{p, v\}$. The left and right transformations are now $N_e \times r$ matrices and can be multiplied to the original second order matrices to get a reduced order model of the same structure. However, for general systems the error bound (29) of this model order reduction approach is lost. To determine the order of the reduced system adaptively, one can monitor the ratio σ_k/σ_1 instead and perform the truncation as soon as the ratio falls below a prescribed tolerance [43].

TABLE I
LEFT AND RIGHT TRANSFORMATIONS MATRICES FOR BALANCED TRUNCATION OF SECOND ORDER SYSTEMS.

type	right transformation	left transformation	SVD
position-position	$V_{pp} := \tilde{R}_p Y_{pp,1} \Sigma_{pp,1}^{-\frac{1}{2}}$	$W_{pp} := \tilde{S}_p X_{pp,1} \Sigma_{pp,1}^{-\frac{1}{2}}$	$X_{pp} \Sigma_{pp} Y_{pp}^T = \tilde{S}_p^T M_e \tilde{R}_p$
position-velocity	$V_{pv} := \tilde{R}_p Y_{pv,1} \Sigma_{pv,1}^{-\frac{1}{2}}$	$W_{pv} := \tilde{S}_v X_{pv,1} \Sigma_{pv,1}^{-\frac{1}{2}}$	$X_{pv} \Sigma_{pv} Y_{pv}^T = \tilde{S}_v^T M_e \tilde{R}_p$
velocity-position	$V_{vp} := \tilde{R}_v Y_{vp,1} \Sigma_{vp,1}^{-\frac{1}{2}}$	$W_{vp} := \tilde{S}_p X_{vp,1} \Sigma_{vp,1}^{-\frac{1}{2}}$	$X_{vp} \Sigma_{vp} Y_{vp}^T = \tilde{S}_p^T M_e \tilde{R}_v$
velocity-velocity	$V_{vv} := \tilde{R}_v Y_{vv,1} \Sigma_{vv,1}^{-\frac{1}{2}}$	$W_{vv} := \tilde{S}_v X_{vv,1} \Sigma_{vv,1}^{-\frac{1}{2}}$	$X_{vv} \Sigma_{vv} Y_{vv}^T = \tilde{S}_v^T M_e \tilde{R}_v$

Since the second order systems discussed here have symmetric and positive definite matrices, it holds $B_e = C_e$, and we have chosen a symmetric equivalent first order system, the balanced truncation approach has some additional properties worth mentioning. At first, because of $P = Q$ and $S = R$ the second order controllability are the same as the observability Gramian matrix, i.e., $P_\xi = Q_\xi$, $\xi \in \{p, v\}$ and the same is obviously true for the associated blocks S_ξ, R_ξ of the low-rank factors. Therefore, the SVDs become EVDs for position-position and velocity-velocity balanced truncation which yields $V_{pp} \equiv W_{pp}$, $V_{vv} \equiv W_{vv}$. This one-sided projections preserve symmetry and positive definiteness of mass, damping and stiffness matrix and hence, both reductions preserve the stability of the original system. This is a similar situation as reported in [41] for position-velocity balanced truncation, where another linearization is used. For the position-velocity and velocity-position approach we also note that, since

$$X_{pv} \Sigma_{pv} Y_{pv}^T = \tilde{R}_v^T M_e \tilde{R}_p = \left(\tilde{R}_p^T M_e \tilde{R}_v \right)^T = Y_{vp} \Sigma_{vp} X_{vp}^T, \quad (41)$$

and it follows $\mathbf{V}_{vp} = \mathbf{W}_{pv}$ and $\mathbf{W}_{vp} = \mathbf{V}_{pv}$, such that by interchanging the right with the left transformation matrix, position-velocity becomes velocity-position balanced truncation and vice versa. This yields, exemplary for the mass matrix, to

$$\widetilde{\mathbf{M}}_{vp} = \mathbf{W}_{vp}^T \mathbf{M}_e \mathbf{V}_{vp} = \mathbf{V}_{pv}^T \mathbf{M}_e \mathbf{W}_{pv} = \widetilde{\mathbf{M}}_{pv}^T \quad (42)$$

such that the reduced mass, damping and stiffness matrices of both approaches are transposes of each other. Moreover, since $\widetilde{\mathbf{B}}_{vp} = \mathbf{W}_{vp}^T \mathbf{B}_e = \mathbf{V}_{pv}^T \mathbf{C}_e^T = \widetilde{\mathbf{C}}_{pv}^T$ and $\widetilde{\mathbf{C}}_{vp} = \widetilde{\mathbf{B}}_{pv}^T$ it follows for the transfer functions of the reduced systems

$$\begin{aligned} \widetilde{\mathbf{H}}_{vp}(s) &= \widetilde{\mathbf{C}}_{vp} \left(s^2 \widetilde{\mathbf{M}}_{vp} + s \widetilde{\mathbf{D}}_{vp} + \widetilde{\mathbf{K}}_{vp} \right)^{-1} \widetilde{\mathbf{B}}_{vp} \\ &= \widetilde{\mathbf{B}}_{pv}^T \left(s^2 \widetilde{\mathbf{M}}_{pv}^T + s \widetilde{\mathbf{D}}_{pv}^T + \widetilde{\mathbf{K}}_{pv}^T \right)^{-1} \widetilde{\mathbf{C}}_{pv}^T = \widetilde{\mathbf{H}}_{pv}(s)^H. \end{aligned} \quad (43)$$

Since complex conjugation and transposition a matrix will not change its maximum singular value, the position-velocity and velocity-position reduced order models share the same frequency response plot in the 2- and Frobenius norms.

Algorithm 4 summarizes the procedure of balanced truncation for the special class of second order systems discussed here using the previously described techniques. For ease of exposition an SVD is used for all balancing types such that the constructions in Algorithm 4 are in line with the ones given in Table I.

Algorithm 4 Balanced truncation for symmetric second order systems

Input: $\mathbf{M}_e, \mathbf{D}_e, \mathbf{K}_e, \mathbf{B}_e, \mathbf{C}_e = \mathbf{B}_e^T$ defining (9), $\nu, \xi \in \{p, v\}$ to define balancing type.

Output: Matrices $\widetilde{\mathbf{M}}_e, \widetilde{\mathbf{D}}_e, \widetilde{\mathbf{K}}_e, \widetilde{\mathbf{B}}, \widetilde{\mathbf{C}}$ of reduced system

- 1: Compute (low-rank) Cholesky factor \mathbf{R} of the solution of (26) using Algorithm 3.
- 2: Compute and partition a (thin) singular value decomposition

$$\mathbf{X}_{\nu\xi} \boldsymbol{\Sigma}_{\nu\xi} \mathbf{Y}_{\nu\xi}^T = \begin{bmatrix} \mathbf{X}_{\nu\xi,1} & \mathbf{X}_{\nu\xi,2} \end{bmatrix} \begin{bmatrix} \boldsymbol{\Sigma}_{\nu\xi,1} & \mathbf{0} \\ \mathbf{0} & \boldsymbol{\Sigma}_{\nu\xi,2} \end{bmatrix} \begin{bmatrix} \mathbf{Y}_{\nu\xi,1} & \mathbf{Y}_{\nu\xi,2} \end{bmatrix}^T = \mathbf{R}_\xi^T \mathbf{M}_e \mathbf{R}_\nu.$$

- 3: Construct the transformation matrices $\mathbf{V}_{\nu\xi}$ and $\mathbf{W}_{\nu\xi}$

$$\mathbf{V}_{\nu\xi} := \mathbf{R}_\nu \mathbf{Y}_{\nu\xi,1} \boldsymbol{\Sigma}_{\nu\xi,1}^{-\frac{1}{2}}, \quad \mathbf{W}_{\nu\xi} := \mathbf{R}_\xi \mathbf{X}_{\nu\xi,1} \boldsymbol{\Sigma}_{\nu\xi,1}^{-\frac{1}{2}}.$$

- 4: Generate reduced order realization

$$\widetilde{\mathbf{M}}_e := \mathbf{W}_{\nu\xi}^T \mathbf{M}_e \mathbf{V}_{\nu\xi}, \quad \widetilde{\mathbf{D}}_e := \mathbf{W}_{\nu\xi}^T \mathbf{D}_e \mathbf{V}_{\nu\xi}, \quad \widetilde{\mathbf{K}}_e := \mathbf{W}_{\nu\xi}^T \mathbf{K}_e \mathbf{V}_{\nu\xi}, \quad \widetilde{\mathbf{B}}_e := \mathbf{W}_{\nu\xi}^T \mathbf{B}_e, \quad \widetilde{\mathbf{C}}_e := \mathbf{C}_e \mathbf{V}_{\nu\xi}.$$

4) *Advantages and Disadvantages:* The balanced truncation reduction method for first order systems has some additional advantages like an immediately available error bound (29), see [20], [32], [2], [1]. This error bound is lost for balanced truncation for second order systems. Stability preservation is an advantage of this reduction method, which holds always for the reduction to a first order system and in special cases also for second order systems. Fortunately, the second order dynamical systems used here fall into this category. The solution of one (or two) generalized Lyapunov equations is, due to the high computation effort, the biggest drawback of the reduction process. The presented SO-LRCF-ADI makes an efficient computation of the solutions possible, but since the solution of linear systems with possibly multiple right hand sides is required in each iteration, it is often more expensive than Krylov subspace methods, but still the method of choice for non-dissipative systems. Furthermore, the generation of suitable shift parameters needed for this algorithm is sometimes a formidable task, both from a theoretical and a computational point of view. For instance, if heuristic shifts are used and generated from crude eigenvalue approximations, they might be of bad quality which can deteriorate the convergence speed of the method significantly. The presence of eigenvalues very close to the imaginary axis or of eigenvalues with very large imaginary parts compared to the real parts can also derail convergence. By the use of second order frequency weighted Gramian matrix based reduction techniques [24], [32] the distribution of the loads is taken into account a

priori and very accurate models can be obtained within a predefined frequency range. Hence, using this method only the load distribution, the frequency range of interest and a measure for the desired accuracy have to be provided by the user.

IV. NUMERICAL RESULTS

In Section II the theoretical background of EMBS together with the important equations have been shown and in Section III a short overview of different reduction techniques have been addressed with a special focus on SVD based reduction techniques. Next some basic aspects of the numerical example, a crank drive with a flexible crankshaft is introduced and the results from reducing the crank drive and the crankshaft will be presented.

A. Combustion Engines with a Flexible Crankshaft

The internal combustion engine is the heart of a vehicle. Shorter development periods and rising requirements like durability, fuel efficiency, mass reduction, noise reduction and the reduction of exhaust gas emission demand precise simulations during the whole design process. For the simulation of combustion engines multi-physics simulations are necessary [39]. The dynamic simulation of a crank drive with elastic parts, transient load curves and the interaction of the components as well as the hydrodynamic coupling of the bearings is a complex issue. The components are loaded dynamically, cyclically and in a multidimensional way. A failure of one key component of the piston engine, e.g. the crankshaft, causes a premature motor fail.

As described in [52], the crank drive is designed to transmit the translational motion, caused by the gas forces that act on the pistons, into rotational movement of the crankshaft. Central elements of the crank drive are the pistons, the piston rods, the crankshaft with the counter-mass like the flywheel and the bearings that connects the crankshaft to the piston rods and the engine block via fluid film lubrications. In Figure 2 a schematic cross-sectional view of the crank drive is drawn, see [6]. The external loads are the combustion gas forces, which act on the pistons and lead to the accessory drive torque on the crankshaft.

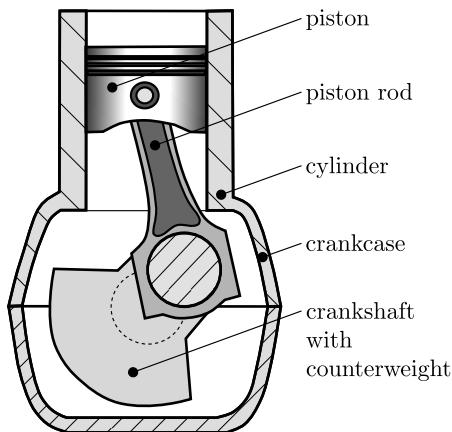


Fig. 2. Structure of a crank drive

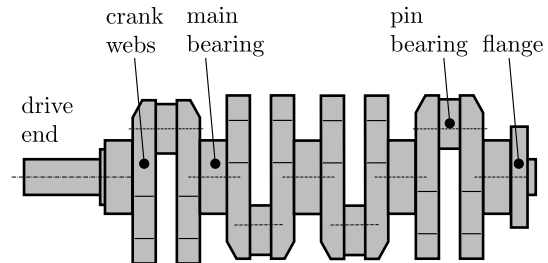


Fig. 3. Crankshaft of a four-cylinder engine

In Figure 3 a crankshaft of a four-cylinder engine is shown. The crankshaft in the figure is designed with balancing weights on the crank webs for compensating the one-sided masses due to e.g. pin bearing or the rotating share of the piston rods. In this work a crankshaft is considered with a rough discretization of $N_e = 51726$ degrees of freedom of the free-free FE model. The loads acting on the crankshaft are distributed over a spatial region of the bearings. In order not to pay attention to every node on the surface of the bearing cones, the coupling of the crankshaft is designed by interface nodes [21], [38]. The reduction results are shown for a crankshaft with rigid elements coupling the interface nodes (RBE2 or CERIG as they are called in the FE packages Nastran and Ansys). Consequently, the matrices of the constraint model are of dimension $N_e = 42126$. The degrees of freedom of the defined interface nodes are taken partly as inputs and outputs at the same time. In total, 35 inputs and outputs are defined, each radial, translatory degree of freedom at the pin bearings, the translatory degree of freedom at the main bearings and all degrees of freedom at the drive end and the flange.

The model of the crank drive and the crankshaft that is analyzed in this investigation was developed within the FVV project 'Low Friction Power Train' and is kindly provided by the 'Lehrstuhl für Maschinenelemente und Tribologie' (IMK), University of Kassel. In the elastic multibody model of the crank drive the crankshaft is considered as flexible and all the other bodies are assumed as rigid. The main bearings which connect the crankshaft to the rigid housing are modeled by five impedance bearings. At the drive end a torsion damper is fixed. In addition, a dual mass flywheel is connected to the crankshaft at the other end of the crankshaft. A Fast Fourier Transformation (FFT) analysis of the signals, acting on the crankshaft in the crank drive, revealed a mainly interesting frequency range from $f = 0$ to about $f = 720$ Hz, see [39].

B. Role of Tribological Applications of the Combustion Engine

The consideration of coupling laws between the elements of the combustion engine is a very complex issue, see e.g. [28]. Such tribological contacts describe the relative motion between solids which are separated by fluid film lubrication. In the combustion engine many contacting parts exist, such as the main bearings or the rod bearings.

As described in [29], a trend to include hydrodynamic interaction in the simulation can be found. This means additional calculations of the load transmission in the feedback system, e.g. at the lubrication gap. Therefore, the calculation of the hydrodynamic pressure distribution based on the hydrodynamic lubrication theory and the determination of the changes in lubrication geometry caused by the position and deformation of the components is necessary. Established characteristic quantities are the minimum gap and the maximum pressure in the bearings. The lubrication geometry requires to consider the elasticity of the components for a realistic calculation of the bearings with fluid film lubrication. This explains the double solving expense for the hydrodynamic equations and the equations of motion of the EMBS. In Figure 4 the different maximum pressures inside the bearings concerning the rigid and elastic crankshaft are shown. The difference makes it obvious that an elastic description is required. The great influence of the deformation of the crankshaft and additionally the deformation of the entire engine block can then be investigated. These differences require to combine hydrodynamic bearings and elastic multibody systems.

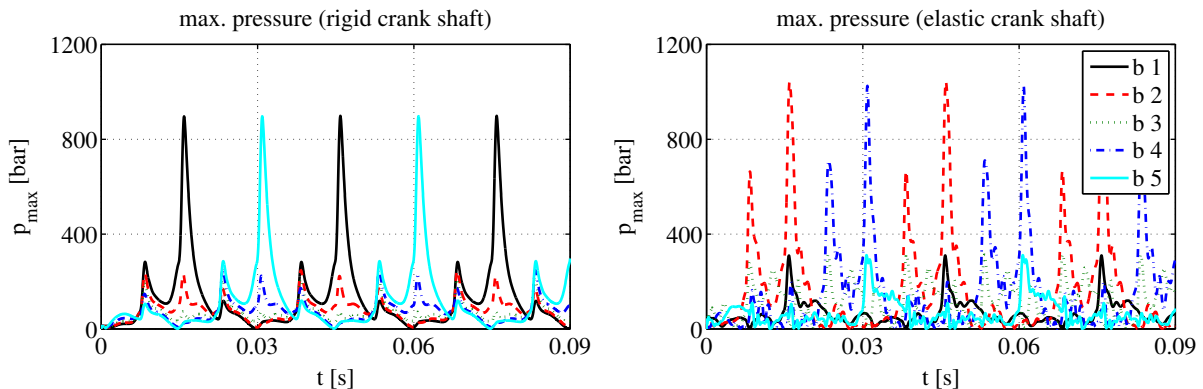


Fig. 4. Maximum pressure in a hydrodynamic bearing (left: rigid, right: elastic) crankshaft

To analyze the pressure p build-up in the hydrodynamic bearings, different methods are available, see [28], [29]. One efficient method is the use of characteristic diagrams of the rigid sliding surfaces. It is qualified for analyses where the complex over-all dynamics of the engine block is in the focus. This method is used for the simulation of the examined EMBS of the crank drive in the FVV project.

C. Frequency Domain Analysis

The criterion to evaluate the effect of the reduction is in the following the relative approximation error

$$\epsilon(s) = \frac{\|\mathbf{H}(s) - \widetilde{\mathbf{H}}(s)\|_F}{\|\mathbf{H}(s)\|_F}, \quad \hat{\epsilon}(s) = \frac{\|\mathbf{H}(s) - \widetilde{\mathbf{G}}(s)\|_F}{\|\mathbf{H}(s)\|_F} \quad (44)$$

in the Frobenius norm. Here, the transfer function matrix of the original system \mathbf{H} is calculated as reference in the frequency domain and is compared with the transfer function matrices

$$\widetilde{\mathbf{H}}(s) := \widetilde{\mathbf{C}}_e \left(s^2 \widetilde{\mathbf{M}}_e + s \widetilde{\mathbf{D}}_e + \widetilde{\mathbf{K}}_e \right)^{-1} \widetilde{\mathbf{B}}_e \quad \text{and} \quad \widetilde{\mathbf{G}}(s) := \widetilde{\mathbf{C}} \left(s \widetilde{\mathbf{E}} + \widetilde{\mathbf{A}} \right)^{-1} \widetilde{\mathbf{B}} \quad (45)$$

of the reduced second and first order model, respectively.

1) *Balanced Truncation Reduced Order Models:* At first the results of balanced truncation are presented. For applying the model order reduction approach of Section III-C the LRCF \mathbf{R} of the Lyapunov equation was obtained with 15 steps of SO-LRCF-ADI (Algorithm 3). The shift parameters were computed using $k_+ = 45$ and $k_- = 35$ Ritz values of $E^{-1}A$ and $A^{-1}E$, respectively. To circumvent additional numerical instabilities in the solution of the linear systems involving $\mu^2 M - \mu D + K$ we neglected all parameters which are greater than 10^5 in magnitude, resulting in $J = 12$ heuristic shifts in total. Since it turned out that even the computed singular values obtained in Algorithm 4 were smaller than any realistic truncation tolerance, see Figure 5, the dimension of the reduced order models was fixed to $n = 70$. Additionally, the system was reduced to a generalized first order system of dimension $n = 140$ using an adequately adapted variant of Algorithm 1. Figure 6 shows the relative error of reduced crankshafts over a frequency range from 0 Hz to 750 Hz. The reduction from second to first order is denoted by *s2f BT*.

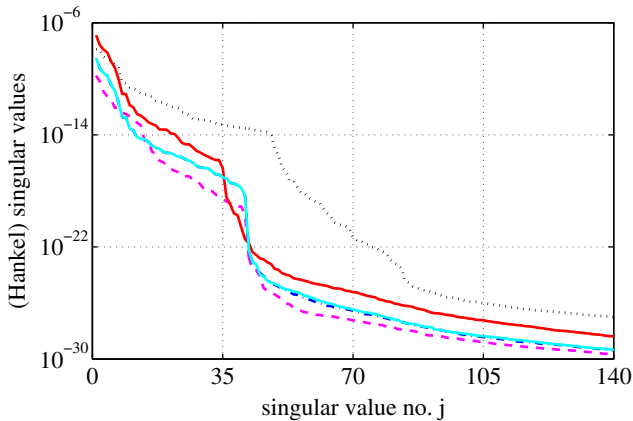


Fig. 5. Decay of the computed singular values

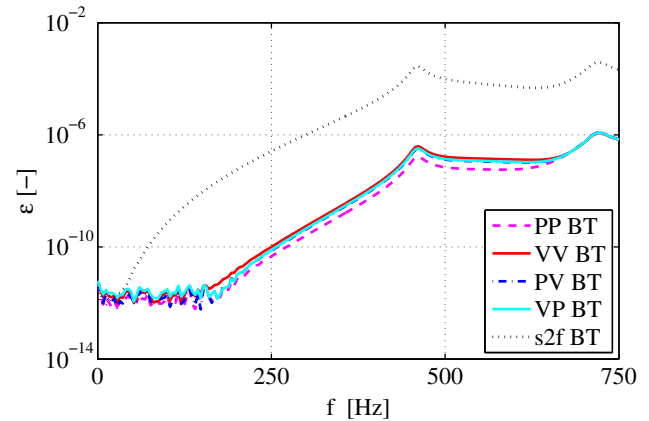


Fig. 6. Relative error of balanced truncation reduced order models

The relative error plots reveal that the accuracy of the reduced second order systems obtained with Algorithm 4 is higher than of the one obtained from the reduction to a first order system. All reduced order models show an increasing relative error as the frequency increases which is a frequently observed phenomenon resulting from the inexact solution of the Lyapunov equations. Note also the consistency of the singular values and relative errors of the position-velocity and velocity-position reduced order model.

2) *Different Reduced Order Models:* For comparison Figure 7 shows the relative error of the reduced order models obtained with the other reduction techniques introduced in Section III. The crankshaft is reduced to the same reduced size of 70.

The Craig Bampton reduction is built by 35 static ansatz functions, representing the number of inputs or outputs respectively, and the same number of internal modes. As the location of the expansion points for the Krylov reduction, which is indicated clearly by the very small relative error in the figure, a frequency of $f = 668$ Hz with a strong amplitude in the flywheel torque, compare [39], is taken. In the reduction with the tangential Krylov method, whereby in principle an increased number of expansion points can be matched in contrast to the standard Krylov reduction, the shifts are equally distributed over a frequency range from 0 to 720 Hz and random complex vectors were used a tangential directions. Clearly, the conventional reduction approaches Craig Bampton and model truncation cannot compete with respect to accuracy with balanced truncation and both Krylov subspace methods. As expected, the Krylov subspace methods achieves its lowest error around the used interpolation point. The tangential interpolation method has the lowest error in the most parts of the considered frequency domain among all reduction methods. Close to the origin the position-position balanced truncation model is more accurate for small frequencies until $f \approx 170$ Hz.

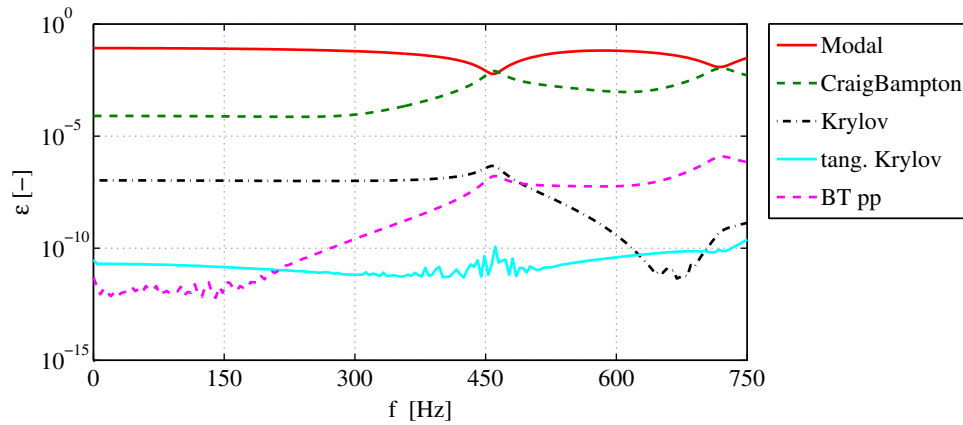


Fig. 7. Relative errors of the different model reduction methods.

V. CONCLUSIONS

The combustion engine and the engine components are examples for a technical system where it is getting more and more important to simulate and optimize efficiently. For realistic simulations of such systems elastic effects can not be neglected. It is shown that the deformation of the crankshaft is of great influence. For the simulation of a crank drive the linear model reduction of the elastic degrees of freedom and so of the crankshaft is a key step. The quality of the reduced models depends decisively on the chosen reduction method. In this contribution some reduction techniques are introduced and the balanced truncation model order reduction is emphasized. The potential of modern reduction techniques is shown by a comparison of different reductions to the same reduced size. Substantial benefits in the relative error can be gained for all modern reduction techniques. In addition, error bounds are available for the non-modal reduction techniques which allows for a more automated model reduction process.

Acknowledgements The authors want to thank the FVV (Forschungsvereinigung Verbrennungskraftmaschinen e.V.) and its working group 'Optimale FE Reduktion' for providing partially the funding for this research and giving us the opportunity to work on these interesting mechanical industrial problems. We also want to thank our project partners Prof. G. Knoll and Dipl.-Ing. G. Ochse from IMK, University of Kassel for their valuable contributions in setting up the mechanical model and the coupling to Tower. Furthermore, we thank our project partner Jens Saak from the Max Planck Institute Magdeburg for crucial assistance regarding the ADI method.

REFERENCES

- [1] A.C. Antoulas and D.C. Sorensen, Approximation of large-scale dynamical systems: An overview, *International Journal of Applied Mathematics and Computer Science* **11**(5), 1093–1121 (2001). 7, 12
- [2] A. Antoulas, *Approximation of Large-Scale Dynamical Systems* (SIAM, Philadelphia, 2005). 1, 4, 6, 12
- [3] M. Arnold and W. Schiehlen (eds.), *Simulation Techniques for Applied Dynamics*, CISM International Centre for Mechanical Sciences, Vol. 507 (Springer, Vienna, 2009). 1
- [4] Z. Bai and Y. Su, Dimension reduction of large-scale second-order dynamical systems via a second-order Arnoldi method, *SIAM Journal on Scientific Computing* **26**, 1692–1709 (2005). 6
- [5] Z. Bai and Y. Su, SOAR: A second-order Arnoldi method for the solution of the quadratic eigenvalue problem, *SIAM Journal on Matrix Analysis and Applications* **26**(3), 640–659 (2005). 6
- [6] M. Bargende, *Verbrennungsmotoren 1* (in German), Vorlesungsskript, Universität Stuttgart, WS 2006. 13
- [7] R.H. Bartels and G.W. Stewart, Solution of the matrix equation $AX + XB = C$ [F4], *Communications of the ACM* **15**(9), 820–826 (1972). 8
- [8] P. Benner, Solving large-scale control problems, *IEEE Control Systems Magazine* **14**(1), 44–59 (2004). 7, 8
- [9] P. Benner, Numerical linear algebra for model reduction in control and simulation, *GAMM Mitteilungen* **29**(2), 275–296 (2006). 4
- [10] P. Benner, P. Kürschner, and J. Saak, Efficient handling of complex shift parameters in the low-rank Cholesky factor ADI method, Tech. rep., Max Planck Institute Magdeburg Preprint MPIMD/11-08, October, 2011, available at <http://www.mpi-magdeburg.mpg.de/preprints/2011/MPIMD11-08.pdf>. 9, 10
- [11] P. Benner, J.R. Li, and T. Penzl, Numerical solution of large Lyapunov equations, Riccati equations, and linear-quadratic control problems, *Linear Algebra and its Applications*, **15**(9), 755–777 (2008). 8, 9, 10
- [12] P. Benner and J. Saak, Efficient Balancing based MOR for second order systems arising in control of machine tools, in: *Proceedings of the MathMod 2009*, edited by I. Troch and F. Breitenecker, ARGESIM Reports Vol. 35 (2009), pp. 1232–1243. 8, 10
- [13] P. Benner and J. Saak, Efficient balancing based MOR for large scale second order systems, *Mathematical and Computer Modelling of Dynamical Systems* **17**(2), 123–143 (2011). 7, 9, 10
- [14] Y. Chahlaoui, D. Lemonnier, A. Vandendorpe, and P.V. Dooren, Second-order balanced truncation, *Linear Algebra and its Application* **415**(2–3), 378–384 (2006). 10
- [15] R. Craig, Coupling of substructures for dynamic analyses: An overview, in: *Proceedings of the AIAA Dynamics Specialists Conference*, Paper-ID 2000-1573, Atlanta, USA, April 5, (2000). 5
- [16] R. Craig and M. Bampton, Coupling of Substructures for Dynamic Analyses, *AIAA Journal* **6**(7), 1313–1319 (1968). 5
- [17] C. Daniel, E. Woschke, and J. Strackeljan, Integration von Tribosystemen in MKS-Modelle am Beispiel von Motorkomponenten (in German), in: *Tagungsband der Magdeburger Maschinenbau-Tage*, (2007).
- [18] I. Duff, A. Erisman, and J. Reid, *Direct methods for sparse matrices* (Oxford University Press, New York, USA, 1986). 9
- [19] J. Fehr, *Automated and Error-controlled Model Reduction in Elastic Multibody Systems*, Dissertation, Schriften aus dem Institut für Technische und Numerische Mechanik der Universität Stuttgart, Band 21 (Shaker Verlag, Aachen, 2011). 4
- [20] J. Fehr and P. Eberhard, Error-controlled Model Reduction in Flexible Multibody Dynamics, *Journal of Computational and Nonlinear Dynamics* **5**(3), 031005–1– 031005–8 (2010). 3, 12
- [21] J. Fehr and P. Eberhard, Simulation Process of Flexible Multibody Systems with Non-modal Model Order Reduction Techniques, *Multibody System Dynamics* **25**(3), 313–334 (2011). 1, 13
- [22] J. Fehr, C. Tobias, and P. Eberhard, Automated and Error-controlled Model Reduction for Durability Based Structural Optimization of Mechanical Systems, in: *Proceedings of the 5th Asian Conference on Multibody Dynamics*, Kyoto, Japan, August 23-26, (2010). 6
- [23] K. Gallivan, A. Vandendorpe, and P. Van Dooren, Model reduction of MIMO systems via tangential interpolation, *SIAM Journal on Matrix Analysis and Applications* **26**(2), 328–349, (2004). 6
- [24] W. Gawronski and J. Juang, Model reduction in limited time and frequency intervals, *International Journal on Systems Science* **21**(1), 349–376, (1990). 12
- [25] L. Grasedyck, Existence of a low rank or H -matrix approximant to the solution of a Sylvester equation, *Numerical Linear Algebra with Applications* **11**, 371–389 (2004). 8
- [26] E. Grimme, *Krylov Projection Method for Model Reduction*, Phd thesis, University of Illinois at Urbana-Champaign, 1997. 1, 4, 5, 6
- [27] S. Hammarling, Numerical solution of the stable, nonnegative definite Lyapunov equation, *IMA Journal of Numerical Analysis* **2**(3), 303–323 (1982). 8
- [28] G. Knoll, J. Lang, and R. Schönen, *Strukturdynamik von Kurbelwelle und Motorblock mit elasto-hydrodynamischer Grundlagerkopplung* (in German), in: *VDI Fortschritt-Berichte, Reihe 11 Schwingungstechnik*, , No. No. 201 (VDI-Verlag and Dissertation RWTH Aachen, 1993). 14
- [29] G. Knoll, R. Lechtape-Güteer, R. Schönen, C. Träbing, and J. Lange, *Simulationstools für strukturdynamische/elasto-hydrodynamisch gekoppelte Motorkomponenten* (in German), FB 15, Institut für Maschinenelemente und Konstruktionstechnik, Universität GH Kassel, Kassel, Januar 2000. 14
- [30] P. Koutsovasilis and M. Beitelschmidt, Comparison of Model Reduction Techniques for Large Mechanical Systems, *Multibody System Dynamics* **20**(2), 111–128 (2008). 5
- [31] P. Leger and E. Wilson, Modal summation methods for structural dynamic computations, *Earthquake Engineering and Structural Dynamics* **16** 1, 23–277 (1988). 5
- [32] M. Lehner, *Modellreduktion in elastischen Mehrkörpersystemen* (in German), Dissertation, Schriften aus dem Institut für Technische und Numerische Mechanik der Universität Stuttgart, Band 10 (Shaker Verlag, Aachen, 2007). 1, 3, 4, 5, 12
- [33] M. Lehner and P. Eberhard, *Modellreduktion in elastischen Mehrkörpersystemen* (in German), in: *Automatisierungstechnik* **54**, 170–177 (2006). 3, 4
- [34] J.R. Li and J. White, Low rank solution of Lyapunov equations, *SIAM Journal on Matrix Analysis and Applications* **24**(1), 260–280 (2002). 8

- [35] J. Lienemann, Complexity Reduction Techniques for Advanced MEMS Actuators Simulation, doctoral thesis, Albert-Ludwigs-Universität Freiburg, 2006. [5](#)
- [36] D. G. Meyer and S. Srinivasan, Balancing and model reduction for second-order form linear systems, *IEEE Transactions on Automatic Control* **41**(11), 1632–1644 (1996). [10](#)
- [37] B. C. Moore, Principal component analysis in linear systems: controllability, observability, and model reduction. *IEEE Transactions on Automated Control*, **AC-26**(1), 17–32, (1981). [1](#), [6](#)
- [38] C. Nowakowski, J. Fehr, and P. Eberhard, Einfluß von Schnittstellenmodellierungen bei der Reduktion elastischer Mehrkörpersysteme, *at - Automatisierungstechnik* **59**(8), 512–519 (2011). [13](#)
- [39] C. Nowakowski, J. Fehr, and P. Eberhard, Model reduction for a crankshaft used in coupled simulations of engines, in: *Proceedings of the ECCOMAS Thematic Conference on Multibody Dynamics 2011*, Brussels, Belgium, (2011). [13](#), [14](#), [15](#)
- [40] T. Penzl, A cyclic low-rank Smith method for large sparse Lyapunov equations, *SIAM Journal on Scientific Computing* **21**(4), 1401–1418 (1999). [8](#)
- [41] T. Reis and T. Stykel, Balanced truncation model reduction of second-order systems, *Mathematical and Computer Modelling of Dynamical Systems* **14**(5), 391–406 (2008). [10](#), [11](#)
- [42] J. Saad, *Iterative Methods for Sparse Linear Systems*, 2 edition (SIAM, Philadelphia, 2003). [4](#)
- [43] J. Saak, *Efficient Numerical Solution of Large Scale Algebraic Matrix Equations in PDE Control and Model Order Reduction*, doctoral thesis, TU Chemnitz, July 2009. [7](#), [8](#), [9](#), [10](#), [11](#)
- [44] B. Salimbahrami and B. Lohmann, Order reduction of large scale second-order systems using Krylov subspace methods, *Linear Algebra and its Applications* **415**(2-3), 385–405 (2006). [6](#)
- [45] W. Schiehlen and P. Eberhard, *Technische Dynamik* (in German) (Vieweg+Teubner, Wiesbaden, 2012). [2](#)
- [46] W. Schilders, H. van der Vorst, and J. Rommes (eds.), *Model Order Reduction: Theory, Research Aspects and Applications*, *Mathematics in Industry*, Vol. 13 (Springer, Berlin, 2008). [1](#)
- [47] R. Schwertassek and O. Wallrapp, *Dynamik flexibler Mehrkörpersysteme* (in German) (Vieweg, Braunschweig, 1999). [2](#), [3](#)
- [48] A. A. Shabana, Flexible multibody dynamics: Review of past and recent developments, *Multibody System Dynamics* **1**(2), 159–223 (1997). [2](#)
- [49] V. Simoncini, A new iterative method for solving large-scale Lyapunov matrix equations, *SIAM Journal on Scientific Computing*, **29**(3), 1268–1288 (2007). [8](#), [9](#)
- [50] D. Sorensen and Y. Zhou, Bounds on eigenvalue decay rates and sensitivity of solutions to Lyapunov equations, Tech. rep. tr02-07, Dept. of Computational and Applied Mathematics, Houston, Hune 2002. [8](#)
- [51] F. Tisseur and K. Meerbergen, The quadratic eigenvalue problem, *SIAM Review* **43**(2), 235–286 (2001). [9](#)
- [52] R. van Basshuysen and F. Schäfer (eds.), *Lexikon Motorentechnik, Der Verbrennungsmotor von A-Z* (in German) (Vieweg, Wiesbaden, April 2004). [13](#)
- [53] R. van Basshuysen and F. Schäfer (eds.), *Handbuch Verbrennungsmotor, Grundlagen, Komponenten, Systeme, Perspektiven* (in German) (Vieweg Teubner, Wiesbaden, 2010).
- [54] E. Wachspress, Iterative solution of the Lyapunov matrix equation, *Applied Mathematics Letters* **107**, 87–90 (1988). [8](#)
- [55] E. Wachspress, *The ADI model problem*, (E.L. Wachspress, Windsor, CA, 1995) [8](#)
- [56] K. Willner, *Methode der finiten Elemente*. (Vorlesungsskript, Universität Stuttgart, Institut A für Mechanik, 1999). [3](#)
- [57] B. Yan, S. X. D. Tan, and B. McGaughy, Second-order balanced truncation for passive-order reduction of RLCK circuits, *IEEE Transaction on Circuit and System II* **55**(9), 942–946 (2008). [10](#)
- [58] S. Zima, *Kurbeltriebe: Konstruktion, Berechnung und Erprobung von den Anfängen bis heute* (in German) (Vieweg, Wiesbaden, 1999).